

## Energy Analysis in a Vapor Compression Refrigeration System Using R32 Refrigerant

Hasanudin<sup>1</sup>, Ananda Duta Suhendar<sup>1</sup>, Amri Abdulah<sup>1</sup>, Renata Lintang Azizah<sup>2\*</sup>, Murtalim<sup>3</sup>, Khoirudin<sup>3</sup>, Karyadi<sup>3</sup>, Abduh Al Afgani<sup>3</sup>

<sup>1</sup>Department of Mechanical Engineering, Sekolah Tinggi Teknologi Wastukencana, Purwakarta, West Java Indonesia, 41151.

<sup>2</sup>Department of Mechanical Engineering Education, Faculty of Technology and Vocational Education Universitas Pendidikan Indonesia, West Java, Indonesia, 40154.

<sup>3</sup>Department of Mechanical Engineering, Faculty of Engineering Universitas Buana Perjuangan Karawang, West Java Indonesia, 41361.

### ABSTRACT

This article reports the results of a study into the efficiency of refrigeration systems. The efficiency of the refrigerant-based cooling system is a significant issue due to its connection to global warming. Vapour compression refrigeration (VCR) systems utilise the inverted Rankine cycle to provide cooling process. Existing systems are evaluated and controlled, and their efficacy is either maintained or improved. A VCR device explores evaporator load variations at five different rpm levels as test equipment for measuring the performance coefficient of R32 refrigerant. A 365-watt compressor drives the VCR system. R32 is a more eco-friendly alternative to R22 as a refrigerant. Interpolation and extrapolation were utilized and adapted to convert the system's experimental enthalpy value to total performance. Genetron was chosen to evaluate enthalpy alongside other factors, such as VCR performance. Genetron properties was used to double-check the experiment's findings. The highest CoP was found and evaluated at a speed of 400 rpm (1<sup>st</sup> level) with the result about 3.17. The lowest value for CoP was found and achieved at the maximum attainable rpm, which was 2.53. The association between CoP and fan speed is inversely proportional during evaporator loading. Genetron properties software validation results produced an average CoP value of less than 10% compared to experimental data. In addition, this work significantly contributes to the study of VCR performance through the development of test devices for the provided VCR system

**Keywords:** *Coefficient of performance, Evaporator, Genetron properties, Refrigerant R32, VCR-system.*

### Article information:

- **Submitted:**  
02/12/2022
- **Revised:**  
25/12/2022
- **Accepted:**  
26/22/2022

### Correspondent Authors:

\*✉:  
[renataliza@upi.edu](mailto:renataliza@upi.edu)

### Type of article:

- ☒ Research papers
- ☐ Review papers

## 1. INTRODUCTION

The government of the Republic of Indonesia has mandated and assessed the implementation of the hydro chlorofluorocarbon phase-out management plan (HPMP) by Ministry of Industry and Trade regulations 41/M-IND/PER/5/2014, 40/M-DAG/PER/7/2014, and 55/M-DAG/PER/9/2014 since 2016.[1]. The Scientific Assessment of Ozone Depletion reported by international agencies NASA, NOAA, UNEP, EC, and WMO determined that R22 has the highest Ozone Depletion Potential (ODP) and Global Warming Potential (GWP) index [2] [3][4]. The Montreal Protocol specifies consumption limits for HCFCs, defined as production plus imports minus exports and destruction, as follows: 1996 (Restrictions limits), 2004 (65%), 2010 (25%), 2015 (10%), and 2020 (0.5%). Developing countries decided to begin phasing out HCFCs in 2013 and are presently implementing a phased-out reduction plan that will conclude in 2030 [5].

The majority of Western and Central European countries accelerated HCFC phase-out. In contrast, most other developed countries mandated the phase-out of R22 by 2010, followed by a restriction on the use of HCFCs in new equipment by 2010 [6]. The timetable for Article 5 countries begins with the freezing of HCFC quantities in 2013 (based on production and consumption levels in 2009–2010), followed by reduction limits of 90%, 65%, 32.5%, and 25%, for 2015, 2020, 2025, and 2030, respectively, and then elimination in 2040 [5] [7]. In commercial and residential air conditioning and heat pump applications, R32 gradually replaces R22, R410A, and other HFC-based refrigerants. There is a 70% reduction in global warming potential (GWP) when R32 is used instead of R410A (GWP = 2088) and a 20% reduction in refrigerant consumption because heat pumps using R32 require only one component to achieve the same cooling capacity as heat pumps using R410A. It increases productivity and reduces costs in the workplace. Since R410A is a compound, it cannot be recycled similarly to R32. R410A may impact home design due to its high operating pressure and the consequent need for higher-pressure compressors and tubing. Refrigerant R410A contains polyester oil, which can degrade when exposed to acid and moisture. The regulations mandate a complete transition from R410A to R32 by 2030 [8]. New regulations could make R32 the standard refrigerant for air conditioning. Eco-friendliness is one of its many advantages. Invest in R32 heat pumps immediately so R32 components can be retrofitted onto R410A heat pumps [9]. There was no mention of air conditioners, heat pumps, or chillers in the SNAP information regarding "unacceptable" or delisted refrigerant categories for R32. It was understandable because there is currently no alternative non-flammable refrigerant available to replace R32 [10].

Several studies conducted and investigated refrigeration systems using alternative fluids, among others, were carried out by [11]. The research introduces a new refrigerant, R422D, as a substitute for R22. This new fluid does not destroy the ozone layer and is compatible with mineral oil but has a high GWP. Experimental analysis confirms that when the system was installed and employed with R422d, it caused an increase in the total equivalent warming impact (TEWI). Further research was carried out by Al-Rashed [12] using four refrigerant fluids, namely R600a, R290, R134a, R32, and R32. The research focused on COP and the evaporator effect, which was carried out and conducted by improving the finned-tube evaporator. The condenser temperature parameter as an independent variable was set and controlled at 38°C and 45°C. The COP values of isobutane (R-600a), urea (R134a), and propane (R290) were higher than those of R22. While R22 has a COP of 9.5%, refrigerants R32 and R410A have a COP of 9.5%. Studies of utilized R32 were also carried out and evaluated by Yashar et al. [13]. They were applied and studied on the RTU (rooftop unit), which has a power of 26.4 kW. The RTU prototype was used and studied to replace the previous evaporator design. The test produced a 2.9, 1.5% increase in COP and a 2.1, 1.5% increase in refrigeration effect. Additionally, the studies utilizing the refrigerant R32 conducted by Sarntichartsak and Thepa [6]. The study investigated the performance of the R32 inverter AC system. Experimental and numerical research methods were utilized and implemented. The parameters used are variations in the frequency of water discharge and spraying temperature. It showed that the proposed model agreed well with the test data.

Although numerous studies on refrigerants have been carried out and evaluated, research on the performance of VCRs using R32 refrigerant validated using Genetron software has been rarely conducted. This article presents the results of an evaporator performance study utilizing the refrigerant R32 in a vapour compression refrigeration (VCR) system with a 365-watt compressor. The experiment was conducted and implemented by varying the speed of the fan's rotation five times, and the experimental method was validated using the Genetron 1.1 software. This study aims to establish the coefficient of performance of R32 fluid at various fan speeds. The energy efficiency of the VCR cycle system with the refrigerant R32 was analysed and evaluated at various sub-cooling levels, evaporator temperatures, and isotropic compressor efficiencies.

## 2. METHODOLOGY

### 2.1. Experimental setup

This experimental test was conducted and done under established safety requirements. Before beginning the experimental testing procedure, all subsystem conditions of the used equipment were inspected and examined to ensure they met safety requirements. Experimental data was collected

using a VCR system with a 365 W compressor and R32 refrigerant. Figure 1 depicts the test plan utilizing VCR system testing equipment.  $T_1$  and  $T_2$  represents the temperature exiting the evaporator or entering the compressor and the temperature exiting the compressor or entering the condenser, respectively.  $P_1$  and  $P_2$  represents the pressure exiting the evaporator or entering the compressor and the pressure exiting the compressor or entering the condenser, respectively. At points  $P_1$  and  $P_2$ , a 500-psi-capacity pressure gauge is installed, while points  $P_3$  and  $P_4$  are calculated based on the refrigerant temperature at points  $T_3$  and  $T_4$ , the data presented in the thermal properties of R32 [12]. Pressure gauges P1 and P2 have an accuracy of 5 psi; if the pressure reading is not exactly on the scale at this resolution, the pressure is determined using the refrigerant R32 properties table. The data were converted and standardized from psi to kPa, where one psi equals 6.89476 kPa. Four glass thermometers were installed and fixed to measure the air temperature entering and exiting the evaporator. They are labelled  $T_{dbE-i}$  and  $T_{dbE-o}$  for the dry bulb temperature entering and exiting the evaporator and  $T_{wbE-i}$  and  $T_{wbE-o}$  for the wet bulb temperature (WBT) in and out of the evaporator. Four glass thermometers were installed and fixed at the air temperature entering and exiting the condenser. They are labelled  $T_{dbC-i}$  and  $T_{dbC-o}$  for the dry bulb temperature (DBT) entering and exiting the condenser and  $T_{wbC-i}$  and  $T_{wbC-o}$  for the wet bulb temperature entering and exiting the condenser. Indoor chamber WBT, DBT, and relative humidity are independent variables [14].

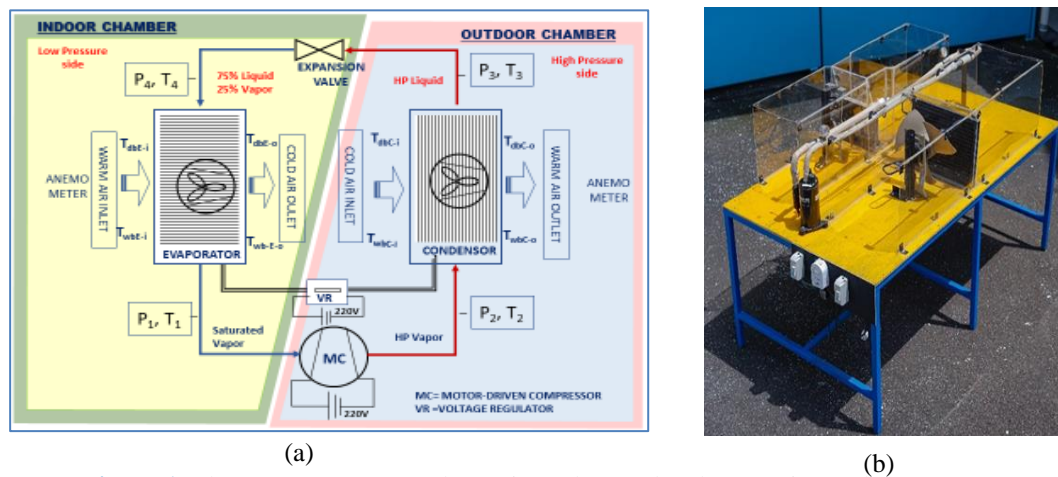


Figure 1. The VCR system: (a) The testing scheme, (b) The experimental set up

## 2.2. Refrigerant R32

The refrigerant R32 has a safety level classification of ASHRAE A1, meaning it has low toxicity levels and is not flammable. Therefore, R22 service tools such as gauge sets, piping, recovery kits, and cylinders can only be used with R32 vehicles if they have been certified for use with them. The R32 system's designers have specified a thicker wall for the compressor and the filter dryer [15]. The operating pressures of gas are crucial for both producers and consumers. New tubing and manometers are required for operation with R32. The new pressures for refrigerants are only slightly greater than those for R410A [16]. Due to the similar operating pressure of the two refrigerants, switching between them is straightforward. The new R32 device may be modelled after the R410A device. R32 has a slightly higher-pressure ratio compared to R410A. The isentropic exponent influences the discharge's pressure ratio and temperature. R32 has an operating pressure between 1200 and 2600 kPa [12]. Significant differences exist between the working pressures of R32 and R410A, but R32 has a greater capacity to exchange heat load, resulting in a greater capacity. Equipment designed for R22 cannot operate with R32 because of pressure differences. It is a compelling argument against upgrading R22 systems to R32 systems and strongly advised that service technicians be certified to handle the higher operating pressures of R32.

Evaluation of a VCR system depends upon refrigerant saturation; the refrigerant's heat flow at its saturation temperature and the system will transform from a liquid to a gas or from a gas to a liquid. Different refrigerants were used in air conditioners. The Montreal Protocol of 1987 and the Kyoto Protocol of 1997 have tightened regulations, mandating the switch to refrigerants with an even more negligible environmental impact [11]. Before recently, R32 was a challenging refrigerant

regarding for changing all R410A to R32 by 2030 would reduce the CO<sub>2</sub> emitted by HFCs by 800 million metric tonnes and it's about 19% in total. For the installation, repair, and maintenance of R32 refrigerant and systems, service methods, working practices, part standards, and occupational safety must be enhanced. Because R32 is combustible and operates at high pressures, manifolds, gauges, vacuum pumps, and recovery units must be evaluated.

### 2.3. Energy Performance.

The evaporator effect test for the VCR system conducted carried out by varying the fan rotation speed. The fan's rotation speed is adjustable across five levels, with each level directly proportional to the fan blades' rpm. In that order, the experiment was implemented and conducted at 400 rpm, 600 rpm, 800 rpm, 1000 rpm, and 1200 rpm. A voltage regulator is installed on the fan wiring system in the evaporator and condenser to control the fan rotation speed. The velocity of air entering the evaporator and condenser is measured using an anemometer. The air ducts for the evaporator and condenser have a cross-sectional area of 0.16 m<sup>2</sup>. The mass flow rate and energy flow through the evaporator and condenser suggested calculated and evaluated using Equations 1 and 2 [10][17].

$$\dot{m}_u = \rho_u \cdot A \cdot v \quad (1)$$

$$Q_u = \dot{m}_u \cdot (h_{in} - h_{out}) \quad (2)$$

Where  $\dot{m}_u$  is the mass flow rate of air in the evaporator or condenser air ducts in kg/s,  $A$  is the cross-sectional area of the evaporator or condenser air ducts in square metres,  $v$  is the air velocity in the evaporator and condenser air ducts in m/s, and  $Q_u$  denotes for energy at the evaporator and condenser inlet and outlet measured in J/kg.

The analysis modeling of the VCR system refers to the first law of thermodynamics, in which the steady-state operation of the process optimizes the energy analysis results. The pipe's pressure drop in components of the VCR system and surroundings is among the untested hypotheses. Changes in the system's kinetic, chemical, and potential energies are disregarded [6] [17]. In a state, several essential thermodynamic properties, such as pressure, temperature, specific gravity, specific volume, enthalpy, entropy, and liquid-vapour properties, will be utilised [9][18]. Compressor of the VCR system generates a pressure differential, allowing refrigerant to flow from one subsystem to the next. The regulator or valve sends refrigerant to the evaporator due to pressure differences between the high and low subsystems. Since the evaporator has a higher refrigerant pressure than the inlet, refrigerant can flow from the evaporator to the compressor through the inlet. In a condenser-evaporator, the refrigerant condition is always a liquid-vapor mixture. The refrigerant's latent properties allow it to absorb and release the same amount of heat as its specific heat, resulting in this condition. During the cycle of the VCR system, refrigerant and lubricant are combined to reduce friction in the installation pipe. **Figure 2** depicts the pressure-enthalpy diagram for the VCR system cycle [19] [20].

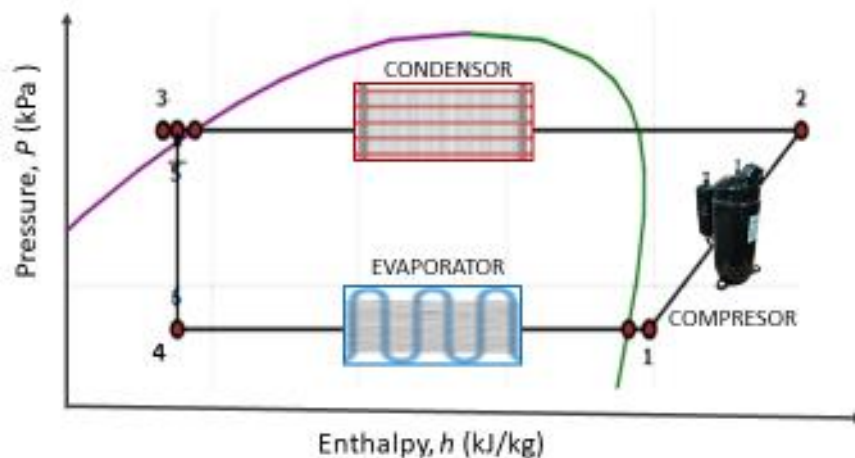


**Figure 2.** Enthalpy-Pressure diagram

Temperature and pressure data for each subsystem were collected during the R32 refrigerant test. The two parameters are used to determine the enthalpy content of each subsystem based on the



thermal properties of R32 [21][22]. When the temperature and pressure are not listed in the enthalpy table, extrapolation or interpolation is used to calculate the enthalpy value. In testing R32 refrigerant with a VCR system, the energy absorbed by the refrigerant is equated to the energy changes in the evaporator and condenser's air ducts. Changes in temperature at the inlet and outlet of the evaporator and condenser indicate changes in energy in the air ducts of the two subsystems. The refrigerant mass flow rate in the evaporator and condenser pipes is determined using equation 3 [23] [24].

$$\dot{m}_{Rfg} = \frac{Q_u}{(h_1-h_4)} = \frac{Q_u}{(h_3-h_2)} \quad (3)$$

Where  $h_1$ ,  $h_2$ ,  $h_3$ , and  $h_4$  represent the enthalpy values at the point of each sub-system described in Figure 2. Meanwhile  $\dot{m}_{Rfg}$  denotes the mass flow rate of refrigerant (kg/s),  $h_1$  and  $h_2$  denote the enthalpy at the point 1 and 2 (kJ/kg). Refrigerant evaporation occurs when the refrigerant passes through the evaporator because the refrigerant absorbs heat from the air in the indoor chamber and increased the refrigerant temperature. Changes in kinetic and potential energy during the evaporation and condensation processes are ignored, so the values of  $v_2^2$  and  $az$  in the compressor sub-system are zero. During the refrigeration cycle, there is no external work on the evaporator and condenser,  $W = 0$ . The rate of energy transfer in the evaporation process can be calculated using equation 4 [24] [17] [25].

$$Q_e = \dot{m}_{Rfg} \cdot (h_1-h_4) \quad (4)$$

Where  $Q_e$  represents the energy absorbed by the refrigerant in the evaporator and represents the work of the evaporation process, which provides a summary of the refrigeration capacity expressed in Watts,  $Rfg$  represents the mass flow rate of the refrigerant in the evaporator in kilograms per second. In contrast,  $h_1$  and  $h_4$  represent the enthalpy values at points 1 and 4, expressed in J/kg. Assuming that isentropic compression in the compressor occurs adiabatically, there is no energy transfer into or out of the compressor as sub-system. The compressor work  $W_c$ , is expressed in J/s or Watts and calculated using Equation 5 [24] [17] [25].

$$W_c = \dot{m}_{Rfg} \cdot (h_2-h_1) \quad (5)$$

The evaporator's heat absorption and the compressor's heat loss can be used to determine the refrigeration effect. Heat absorbed by the evaporator and heat lost to the air are used to determine the refrigeration effect and cooling capacity. The air that passes through the evaporator pipe serves as the cooling load in the experiment. Air's heat-absorption capacity can be calculated using Equation 6 [24] [17] [25].

$$Q_{uc} = \dot{m}_u \cdot C_p \cdot \Delta T_u \quad (6)$$

Where  $Q_{uc}$  represents the magnitude of the refrigeration effect in J/s,  $C_p$  is the heat specific of air under isobaric conditions (constant pressure). It has a value of 0.2403 (kJ/kg. K), and  $R$  is the specific heat of water at constant pressure,  $\dot{m}_u$  represents of air mass flow rate in kg/s, and  $T_u$  represents the change in air temperature passing through the evaporator. The value of  $T_u$  is calculated using equation 1 [26]. At the identified temperature and pressure conditions, the density value of air at a specific temperature can be calculated by equation 7. Heat transfer from the refrigerant to a more excellent environment occurs when it passes through the condenser and produces refrigerant condensation. Equation 8 states the rate of heat transfer in this condensation process [17] [24] [25].

$$\rho = \frac{P}{R \cdot T} \quad (7)$$

$$Q_c = \dot{m}_{Rfg} \cdot (h_2-h_3) \quad (8)$$

Where  $P$  is the absolute pressure of air in N/m<sup>2</sup>,  $R$  is the ideal fluid constant of air at 2.4061 (kJ/kg, K),  $Q_c$  is the rate of energy released into the air during condensation (J/s or W), and  $h_2$  and  $h_3$  are the enthalpies at points 2 and 3, respectively (kJ/kg). It is due to throttling in the capillary tube, which functions as an expansion valve.  $W = 0$  because no external work is performed during the throttling process. Considered to be zero are changes in potential and kinetic energy [26]. Because the process is adiabatic, there is no change in enthalpy, so the enthalpies at points 3 and 4 are considered identical. Equation 10 describes this condition.

$$h_3 = h_4 \quad (10)$$

The sub-VCR system requires mechanical energy from the compressor to circulate the refrigerant to each component. The evaporator extracts heat, which then flows to the condenser. The expansion valve reduces the amount of refrigerant in the condenser to enhance the performance of the evaporator. Here, there is a trade-off between low refrigerant pressure and low temperature and the refrigerant mass flow rate. Equation 11 calculates the VCR system's performance [24] [17] [25].

$$CoP = \frac{Q_e}{W_c} = \frac{\dot{m}_{Rfg} \cdot (h_1 - h_4)}{\dot{m}_{Rfg} \cdot (h_2 - h_1)} = \frac{(h_2 - h_1)}{(h_1 - h_4)} \quad (11)$$

#### 2.4. Software Refrigeration System

Honeywell's Genetron Properties is a refrigeration system programmed validating fluid or mixture state points and cycle calculations[27]. This application offers a flexible user interface for data entry with validation error alerts. The refrigerant input parameter was set and fixed with R32, and the project input parameter was confirmed and set to the Basic Cycle model. The validation input data consist of compressor data, including a cooling load of 1025 watts, an isentropic efficiency of 70%, and a volumetric efficiency of 0.95 per cent. The data regarding the cooling load was derived and provided from the compressor's specifications. Also considered input data are variations in the discharge line temperature, condenser condensing and outlet temperatures, and evaporator evaporating and outlet temperatures. It was confirmed and shown that the discharge line subsystem's condenser, liquid line, evaporator, and suction line components have no pressure drop. **Figure 3** depicts the schematic diagram of VCR system [28][29].

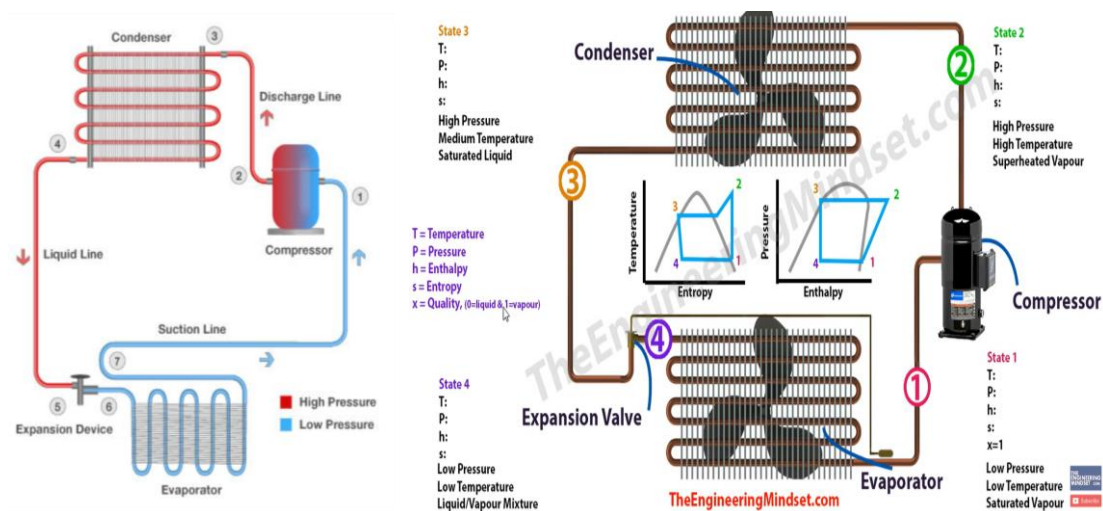


**Figure 3.** Schematic diagram of the VCR system

### 3. RESULT AND DISCUSSION

#### 3.1. Pressure and Temperature Profile

The evaporator and condenser of the VCR system have been installed, along with temperature and pressure monitoring instruments for gathering data on the temperature and pressure of the refrigerant. There were five experimental levels in the experimental set. **Table 1** displays the temperature and pressure measurements that resulted and were provided for the refrigerant in the VCR system during the R32 refrigerant experiment. Temperature and pressure measurements are taken at five test levels on the condenser side. Temperature and pressure measurements obtained during the experiment are used and utilized to compute the enthalpy of each subsystem. The enthalpy calculation will be employed using the R32 refrigerant characteristics table [2]. These data were adopted using numerical interpolation or extrapolation methods, and the Genetron program was used and provided to validate the results. The experimental investigation and software validation outcomes will be used to compare and analyze the completed.

**Table 1.** Temperature and pressure profiles on the evaporator and condenser side

RPM Level	Evaporator-Out		Condenser-In		Condenser-Out		Evaporator-In	
	P <sub>1</sub> (kPa)	T <sub>1</sub> (°C)	P <sub>2</sub> (kPa)	T <sub>2</sub> (°C)	P <sub>3</sub> (kPa)	T <sub>3</sub> (°C)	P <sub>4</sub> (kPa)	T <sub>4</sub> (°C)
1	1109	10.3	3822.3	108.2	3822.3	47.9	1108.6	10.1
2	1054	8.9	4073.3	116.5	4073.3	47.0	1,053.6	8.35
3	989	6.9	3851.9	114.8	3851.9	44.8	988.7	6.25
4	954	6.2	3734.5	114.4	3734.5	43.4	954.4	5.1
5	989	6.9	3851.9	114.8	3851.9	44.8	988.7	6.3
	Saturated Vapour		Superheated Vapour		Saturated Liquid		Liquid /Vapour	

### 3.2. Enthalpy Analysis

Enthalpy measures thermodynamic energy. Enthalpy equals a system's total heat, which is its internal energy multiplied by its volume and pressure. Technically, enthalpy refers to the internal energy required to generate a system and the amount of energy needed to make room for it by establishing its pressure and volume. The refrigerant exits the evaporator and enters the compressor suction valve [25]. All superheat has been removed from this illustration to keep it simple. The second step indicates the refrigerant condition as it exits the compressor and enters the condenser. The refrigerant is superheated right now. The third step verifies the refrigerant as it leaves the condenser and enters the check valve devices. In the fourth step, the refrigerant enters the evaporator as a saturated liquid. Several changes are needed to fix a refrigeration system problem. In this and subsequent examples, temperature refers to the refrigerant, not the condenser or product. Changing liquid refrigerant to a gas at the same temperature is key to the refrigeration cycle. One must absorb enough heat to cause the change. This heat is known as latent heat or heat from vaporization. During the refrigeration cycle, this takes place in the evaporator [30]. There is no other location that effectively cools. The remainder of the apparatus recycles the liquid by condensing the gas first. The horizontal distance separating the saturated liquid line from the saturated vapor line is a good representation of the amount of latent heat present.

The calculation experiment for enthalpy was conducted using the temperature and pressure values from Table 1. Using the R32 thermal properties data, the enthalpy data were then interpolated. Figure 4 depicts the interpolation and extrapolation data for enthalpy values  $h_1$ ,  $h_3$ , and  $h_4$ . In the meantime, Figure 5 illustrates the interpolated and extrapolated data for  $h_2$ .

	kPa	°C	$h_1$	kPa	°C	$h_3=h_4$
1	1105.00	10.30	516.70	3822.3	47.90	292.53
	1140.00	11.00	516.74	3900.00	50.00	297.486
	1174.00	12.00	516.80	4000.00	55.00	309.286
	kPa	°C	$h_1$	kPa	°C	$h_3=h_4$
2	1034.21	8.90	516.56	4073.3	47.00	290.41
	1074.00	9.00	516.57	1074.00	50.00	297.49
	1107.00	10.00	516.66	1107.00	55.00	309.29
	kPa	°C	$h_1$	kPa	°C	$h_3=h_4$
3	999.74	6.90	516.35	3851.9	44.8	285.86
	1012.00	7.00	516.36	1012.00	45.00	286.308
	1043.00	8.00	516.47	1043.00	50.00	297.49
	kPa	°C	$h_1$	kPa	°C	$h_3=h_4$
4	1034.21	6.20	516.27	3734.5	43.40	282.73
	1012.00	7.00	516.36	1012.00	45.00	286.31
	1043.00	8.00	516.47	1043.00	50.00	297.49
	kPa	°C	$h_1$	kPa	°C	$h_1$
5	1034.21	7.80	516.45	3851.9	44.80	285.86
	1043.00	8.00	516.47	4877.00	45.00	286.31
	1074.00	9.00	516.57	1074.00	50.00	297.49

**Figure 4.** The interpolation and extrapolation for enthalpy at  $h_1$ ,  $h_3$  and  $h_4$

Superheated VApor				4058	4881	Superheated VApor				4881	5.826	Superheated VApor				4058	4881
1	3822.3	T1		69.5	69.5	2	4073.3	T1		76	76	3	3851.9	T1		73	73
		T2		70	70			T2		80	80			T2		70	70
		T3		75	75			T3		85	85			T3		75	75
	69.5	h1		575.68	580.69		76.1	h1		586.50	591.19		73.3	h1		578.41	583.32
		h2		576.04	581.04			h2		589.08	593.83			h2		576.0	581.0
		h3		579.63	584.50			h3		592.40	597.23			h3		579.6	584.5

Superheated VApor				4058	4881	Superheated VApor				4881	5.826
4	3734.5	T1		71.9	71.9	5	4805.2	T1		69.3	69.3
		T2		70	70			T2		70	70
		T3		75	75			T3		75	75
	72	h1		577.4	582.35		69.3	h1		580.56	582.11
		h2		576.04	581.04			h2		581.04	582.78
		h3		579.63	584.50			h3		584.50	587.59

Figure 5. The interpolation and extrapolation for enthalpy at  $h_2$ 

### 3.3. Energy Analysis on VCR System

The energy consumption analysis of the VCR system focuses on the appliance's evaporator, condenser, and compressor. According to the principle of energy conservation, the amount of energy absorbed by the refrigerant at the condenser ( $Q_c$ ) must be equal to the amount of energy released into the air by the condenser ( $Q$ ). However, heat loss in the compressor, heat removal in the condenser, and heat absorption in the evaporator differ. Total system work equals the heat removed during condensation [8]. Figure 6 illustrates the energy input to the evaporator (energy absorbed by the evaporator), the work performed by the compressor (heat pump), and the energy output of the condenser. Equation 11 calculates the VCR system's performance at each fan speed. The amount of energy in the evaporator is proportional to the speed at which the fan is rotating. The total energy input and output of a VCR is proportional to the fan speed. In the meantime, the work performed by the pumps increased marginally at rotational speed 2 and thereafter followed a pattern that was predominantly linear with rising the fan speed.

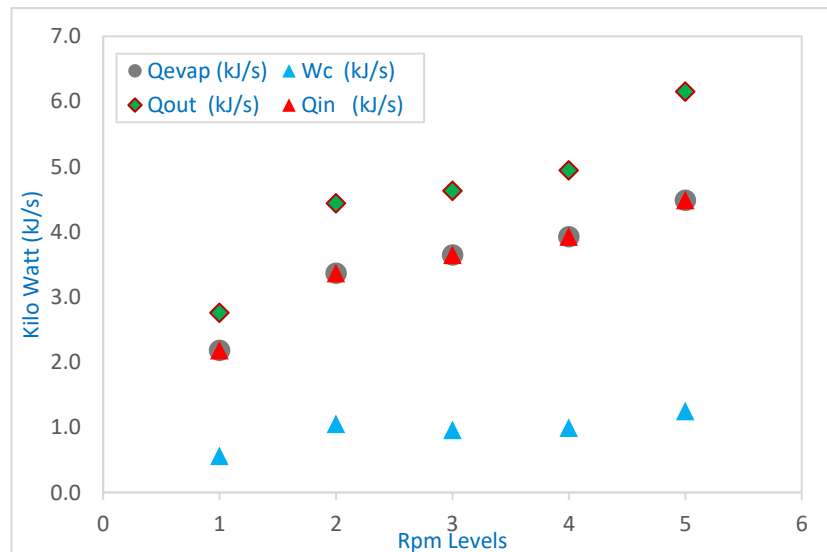


Figure 6. The energy at each sub-system of the VCR system

The performance of the VCR system is depicted in Figure 7 based on theoretical calculations and validation results acquired using Genetron software. The performance of the VCR system using R32 with a performance indicator coefficient getting well between 3.20 and 3.90 for the experimental and 2.53 to 3.17 for software simulations. The finding relates following with the previously research was conducted by Taib et al. [9]. They discovered that a CoP of the VCR system is between 2.75 and 3.50. This research demonstrates a roughly 0.4-point rise in experimental CoP. Although the software validation results are still within the range of the prior research. This study's findings corroborate those of [18], who found that when fan rotation speed increased, the coefficient of



performance (CoP) decreased.

The highest CoP value provided by software validation was recorded at 400 rpm (1<sup>st</sup>- level), where it was 3.17, and the lowest was recorded at 1200 rpm (5<sup>th</sup> levels), where it was 2.503. Whereas, the highest CoP value provided by experimental result was recorded at 400 rpm (1<sup>st</sup>- level), where it was 3.90, and the lowest was recorded at 600 rpm (2<sup>nd</sup> levels), where it was 2.53. The validation results generated by the Genetron 1.1 software were found and achieved to be less than 10 % more valuable than the experimental data.

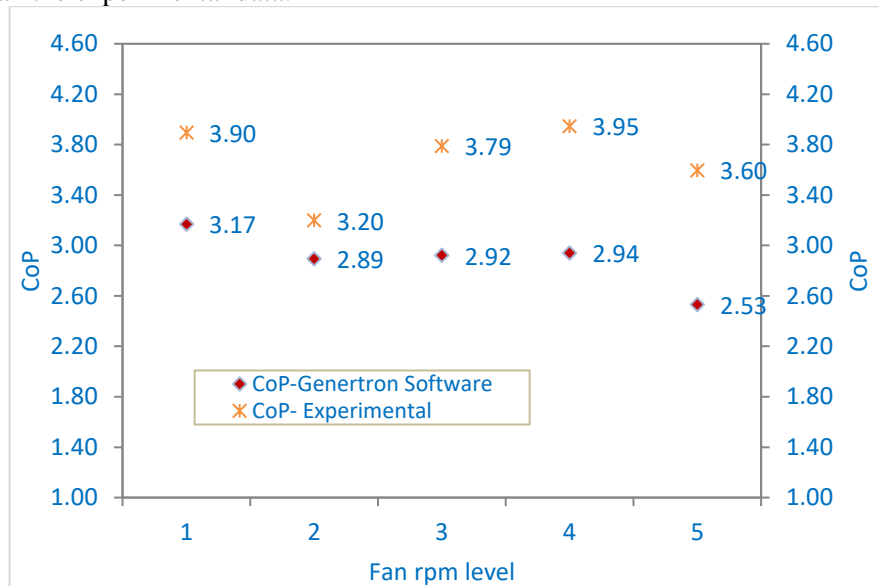


**Figure 7.** Coefficient of performance R32 in the VCR system

#### 4. CONCLUSIONS

The VCR performance with R32 refrigerant has been performed investigated. The following explains the research findings about the use of refrigerant as an environmentally beneficial fluid. The CoP of the experimental result reached about 3.20-3.9. It has higher than compared with the software validation. The CoP value are in direct proportional with the rotation of the fan speed. The CoP will decrease as rotation speed is increased. A VCR with a CoP indication will typically perform worse when the fan speed is increased. It is possible to get accurate results from tests with given reliable test equipment, and the procedure must be parallel with high employability and reliable measuring devices. The efficiency of the R32-refrigerant-using VCR system was analyzed, and its cooling capacities were found to range from 1024 to 1065 watts. In addition, this work significantly contributes to the study of VCR performance through the development of test devices for the provided VCR system.

#### AUTHOR'S DECLARATION

##### Authors' contributions and responsibilities

The authors contributed significantly to the conception and design of the study. The authors were responsible for data analysis, results interpretation, and discussion. The authors read the final manuscript and gave their approval.

##### Availability of data and materials

The authors have made all data available.

##### Competing interests

The authors declare that they have no competing interests.

#### REFERENCE

- [1] Kementerian Perdagangan RI, *PERUBAHAN ATAS PERATURAN MENTERI PERDAGANGAN NOMOR 03/M-DAG/PER/1/2012 TENTANG KETENTUAN IMPOR*

- BAHAN PERUSAK LAPISAN OZON (BPO). Indonesia, 2014.
- [2] World Meteorological Organization, “Scientific Assessment of ozone Depletion: 2018,” 2019. [Online]. Available: <https://ozone.unep.org/sites/default/files/2019-05/SAP-2018-Assessment-report.pdf>
  - [3] NOAA NASA UNEP WMO EC, “Scientific Assessment of ozone Depletion: 2010,” 2010.
  - [4] S. Sukarman, A. Abdullah, and R. H. Rahmanto, “Analisis Kinerja Mesin Pendingin Kompresi Uap Menggunakan HFC-236fa Sebagai Alternatif Pengganti R-22,” *JTERA (Jurnal Teknol. Rekayasa)*, vol. 4, no. 1, p. 131, 2019, doi: 10.31544/jtera.v4.i1.2019.131-138.
  - [5] UNEP, *Decisions adopted by the nineteenth meeting of the parties to the Montreal protocol on substances that deplete the ozone layer. Nairobi, Kenya: United Nations Environment Programme (UNEP) Ozone Secretariat*; 2007.
  - [6] P. Sarntichartsak and S. Thepa, “Modeling and experimental study on the performance of an inverter air conditioner using R-410A with evaporatively cooled condenser,” *Appl. Therm. Eng.*, vol. 51, no. 1–2, pp. 597–610, 2013, doi: 10.1016/j.applthermaleng.2012.08.063.
  - [7] S. Jaime, O. Ignacio, C. Fernando, and Á. Estrella, “Drop-in performance of the low-GWP alternative refrigerants R452B and R454B in an R410A liquid-to-water heat pump,” *Appl. Therm. Eng.*, vol. 182, 2021, doi: <https://doi.org/10.1016/j.applthermaleng.2020.116049>.
  - [8] Environmental Protection Agency, *Federal Register*. USA: <https://www.govinfo.gov/content/pkg/FR-2016-04-18/pdf/2016-08163.pdf>, 2016.
  - [9] ASHRAE, *ASHRAE Handbook: Fundamentals*. Atlanta: ASHRAE: Atlanta, GA, USA, 2013.
  - [10] S. K. Wang, *Handbook of Air Conditioning and Refrigeration*. McGraw-Hill, 2000.
  - [11] C. Aprea and A. Maiorino, “An experimental investigation of the global environmental impact of the R22 retrofit with R422D,” *Energy*, vol. 36, no. 2, pp. 1161–1170, 2011, doi: 10.1016/j.energy.2010.11.032.
  - [12] A. A. A. Al-Rashed, “Effect of evaporator temperature on vapor compression refrigeration system,” *Alexandria Eng. J.*, vol. 50, no. 4, pp. 283–290, 2011, doi: 10.1016/j.aej.2010.08.003.
  - [13] D. A. Yashar, S. Lee, and P. A. Domanski, “Rooftop air-conditioning unit performance improvement using refrigerant circuitry optimization,” *Appl. Therm. Eng.*, vol. 83, pp. 81–87, 2015, doi: 10.1016/j.applthermaleng.2015.03.012.
  - [14] Y. Do et al., “An experimental study on the performance of a condensing tumbler dryer with an air-to-air heat exchanger,” *Korean J. Chem. Eng.*, vol. 30, no. 6, pp. 1195–1200, 2013, doi: 10.1007/s11814-013-0037-4.
  - [15] M. Setiyo, S. Soeparman, N. Hamidi, and S. Wahyudi, “Caractéristiques de l’effet refroidissant d’un système frigorifique à demi-cycle sur un système au GPL,” *Int. J. Refrig.*, vol. 82, pp. 227–237, 2017, doi: 10.1016/j.ijrefrig.2017.06.009.
  - [16] M. Y. Taib, A. A. Aziz, and A. B. S. Alias, “Performance Analysis Of A Domestic Refrigerator,” in *1st NCMER 2010, 26-27 May, 2010*, 2010, vol. 9501, no. May, pp. 582–591. [Online]. Available: <http://umpir.ump.edu.my/1593/>
  - [17] S. K. Wang, *Air-Conditioning and Refrigeration Mechanical Engineering Handbook*.
  - [18] S. Sukarman, K. Khoirudin, M. Murtalim, A. Fauzi, R. Valderama, and A. Abdulah, “Analisis Kinerja Evaporator Pada Vapors Compression Refrigeration System Menggunakan Refrigerant R410a,” *J. Teknol.*, vol. 14, no. 1, pp. 127–138, 2022.
  - [19] M. Kim, W. V. Payne, P. A. Domanski, S. H. Yoon, and C. J. L. Hermes, “Performance of a residential heat pump operating in the cooling mode with single faults imposed,” *Appl. Therm. Eng.*, vol. 29, no. 4, pp. 770–778, 2009, doi: 10.1016/j.applthermaleng.2008.04.009.
  - [20] M. M. Dwinanto and S. Prajitno, “Optimization of a Dual-Evaporator Vapor Compression Refrigerator,” 2018, pp. 181–187.

- [21] Climalife, “Thermodynamic properties of R-32,” 2014.
- [22] KLEA, “Thermodynamic Property Data,” Mexichem, 2010.
- [23] S. W. F, *Refrigersi dan Pengkondisian Udara*. Jakarta: Erlangga, 2005.
- [24] Z. Wang, F. Zheng, and S. Xue, “The economic feasibility of the valorization of water hyacinth for bioethanol production,” *Sustain.*, vol. 11, no. 3, 2019, doi: 10.3390/su11030905.
- [25] Y. A. Cengel and M. A. BOLES, *THERMODYNAMICS: AN ENGINEERING APPROACH*, 6th ed. Singapore: McGraw-Hill, 2007.
- [26] Y. A. Cengel, *Introduction to Thermodynamics and Heat Treansfer*, 2nd ed. McGraw-Hill, 2008.
- [27] S. Sukarman, A. D. Shieddiqie, I. B. Rahardja, A. I. Ramadhan, and Y. Handoyo, “Energy Analysis Of Vapor-Compression Refrigeration ( VCR ) System,” *Int. J. Sci. Technol.*, vol. 8, no. 09, pp. 1285–1289, 2019.
- [28] J. R. Simões-Moreira, “A thermodynamic formulation of the psychrometer constant,” *Meas. Sci. Technol.*, vol. 10, no. 4, pp. 302–311, 1999, doi: 10.1088/0957-0233/10/4/008.
- [29] The Engineering Mindset, *How to DESIGN and ANALYSE a refrigeration system*, (2017). [Online]. Available: <https://www.youtube.com/watch?v=TPabv9iDENc>
- [30] W. F. Stoecker, *Refrigersi dan Pengkondisian Udara*. Erlangga, 2005.